CHAPTER VI

A Combined Experimental and Theoretical Study on *p*-Sulfonatothiacalix[4]arene Encapsulated Sulisobenzone

Abstract : Sunscreen ingredient such as sulisobenzone (SBZ) has the tendency to degrade when exposed to UV-radiation which becomes major problem for their further development and application in cosmetic industry. Host-guest inclusion complexation could be a promising strategy to address this issue. New inclusion system of SBZ with *p*-sulfonatothiacalix[4]arene (TSC4X) was fabricated, and its binding behaviour both in solution and solid states has been investigated by UV-Visible spectroscopy, ^{1}H NMR, DSC, ESI-MS and FT-IR spectroscopy. The 1:1 stoichiometry of the inclusion complex was confirmed by Job plot and mass spectrometry. TSC4X displayed strong affinity for SBZ and the binding process was found to be thermodynamically feasible. FT-IR and ^{1}H NMR spectroscopic studies demonstrated that the unsubstituted aromatic moiety of SBZ is inserted into the cavity of TSC4X, which is in accordance with the molecular docking study. The aqueous solubility, photostability and thermal stability of SBZ were improved on complexation with TSC4X. The molecular docking study depicted the most feasible conformation of inclusion complex with lowest binding energy.

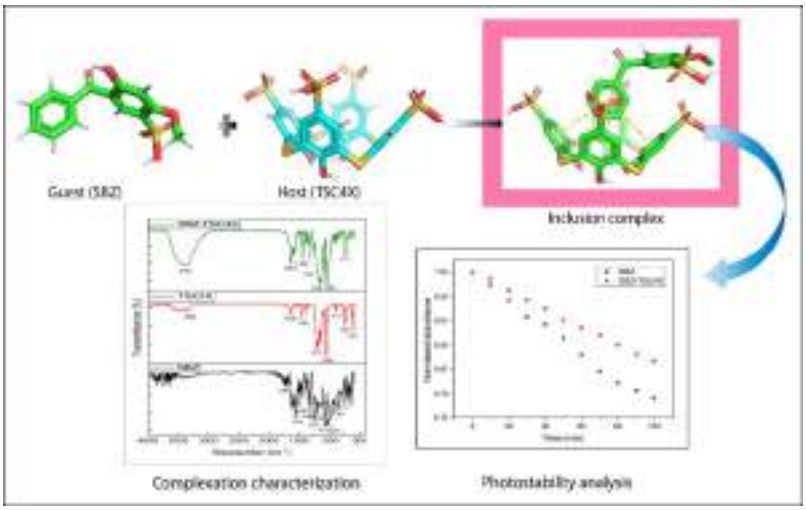

Keywords : Sulisobenzone ; *p*-sulfonatothiacalix[4]arene ; Differential scanning calorimetry ; Photostability ; Solubility ; Molecular docking.

VI.1. Introduction

Human skins are sensitive towards ultraviolet radiations (UVR). Protection of the skin from the sunlight is the prime concern of society.[1] Excessive exposure of skin to the UV radiation leads to various skin related diseases such as skin aging, loss of collagen, stimulating the formation of reactive oxygen species, and can cause DNA damage, inflammatory effects, pigment darkening, immunosuppression, and carcinogenesis.[2,3] However, 7-dehydrocholesterol absorbs UV-B radiation to produce previtamin D3 which successively isomerizes to vitamin D. Thus, underexposure of skin to UV-B can lead to a vitamin D deficiency, which may promote the development of skeletal disease and osteoporosis.[4] Therefore, an increase in the adverse effects of ultraviolet (UV) radiation on the skin encouraged cosmetic formulators to work in the area of UV blockers and their effective means of delivery.[5] Generally, UV-radiation is subdivided into three categories, namely, UVA (near UV radiation with wavelength range 320-400 nm), UVB (UV radiation with wavelength range 280-320 nm) and UVC (far UV radiation with wavelength range 200-280 nm) radiations.[6,7] Many classes of sunscreen agents including organic chemicals such as cinnamates, benzophenones, para-aminobenzoic acid (PABA), camphor derivatives and inorganic chemicals such as titanium dioxide (TiO_2), zinc oxide (ZnO) having great photostability and non-toxicity are used as excellent UV filters or UV blockers.[8-10]

Sulisobenzone (SBZ) is a benzophenone based Food and Drug Administration (FDA) approved broad spectrum sunscreen agent (Scheme 1). It absorbs ultraviolet radiations in both UV-A and UV-B range (wavelength between 280 and 400 nm).[11] Apart from being UV filter, it has shown to act as estrogen, antiestrogen, and antiandrogen in *in vitro* assays.[12] To increase the efficacy of the sunscreen, the formulation of a sunscreen requires the active chemical to penetrate less efficiently and to remain localized close to the skin surface for an extended period. An ideal sunscreen should show a high extent of substantivity at the lowest possible level of transdermal penetration.[13,14]

So, various studies have been carried out with the incorporation of individual organic UV filters into nanocarrier with different materials such as nanoparticles,[15] lignin,[16] liposomes,[17] cyclodextrins,[18] calixarene[19] and ethyl cellulose[20]. Cyclodextrins as well as calixarenes are very appealing as carriers for organic UV filters because of their

biodegradability, biocompatibility, ability to improve the photostability of UV filters and suitability in various solvent systems, which makes them useful for different pharmaceutical formulations.[21] They act as a carrier through molecular encapsulation and enhances the cosmetic formulations therapeutic effect by stabilizing the photosensitive drugs.[22]

Unlike calixarene, thiacalixarenes are a class of macrocycles having π-electron-rich aromatic moieties composed of phenol units linked by sulphur instead of methylene bridges.[23] The *p*-sulfonatothiacalix[4]arene (TSC4X) can be used to form supramolecular complex due to its high water solubility, wider hydrophobic cavity, lower electron density, more flexibility and additional coordination sites (S-atom) [Scheme 1].[24] It also has enormous applications in the fields of drug delivery, supramolecular amphiphiles, chemical sensors, enzyme mimic/enzyme assay, metal complexation, biomedicine, etc.[25-27] Encapsulation of sunscreens within different macrocyclic hosts to form stable inclusion complexes have been investigated in the last decades.[28] Now-a-days, a large number of complexes have been commercialized due to useful applications in many fields, ranging from cosmetics industry to inks technology and fabrics, with enhanced properties with respect to great protoprotection, photostability, water solubility, and skin penetration.[29,30]

In the present study, we have reported the preparation of inclusion complex of TSC4X with the sunscreen SBZ by mechanochemical method. The prepared complex was characterized by UV-visible spectroscopy, ^{1}H NMR, DSC analysis, FT-IR spectroscopy and ESI-MS study. Molecular docking study was conducted as well to get a deep insight on the orientation of SBZ into the TSC4X cavity. Finally, the aqueous solubility, thermal stability and photostability of the complex have also been investigated.

VI.2. Experimental section

VI.2.1. Materials

Both sulisobenzone and *p*-sulfonatothiacalix[4]arene were procured from TCI Chemicals Pvt. Ltd (India). The purity of sulisobenzone and *p*-sulfonatothiacalix[4]arene were >98%. Doubly distilled water was used in all experiments.

VI.2.2. Instruments

All the UV-Visible spectroscopic studies were carried out in Agilent 8453 UV-Visible spectrophotometer with uncertainty ±2 nm where a quartz cell (1 cm×1 cm×4 cm) with a conventional 1 cm path length has been used.

The KBr disk technique was employed to record Fourier Transform Infrared (FT-IR) spectra by Perkin Elmer spectrometer in the wavenumber range 4000-400 cm^{-1} with a 2 cm^{-1} resolution. The sample and KBr were taken in the ratio of 1:100 to prepare the disks.

Solution state ^{1}H NMR experiments were performed on Bruker Avance 300 MHz NMR spectrometer using D_2O as a solvent at 298.15 K. The residual D_2O peak was taken as an internal standard.

The mass characterization was performed using electrospray ionization mass spectrometer (ESI–MS) in positive mode with scan range 0-1200 m/z. The solution (90 : 10) water : methanol was thoroughly used with the flow being 0.120 ml/min.

All the DSC spectra were recorded using Perkin Elmer Pyris DSC 6. Heating of 1.2 mg of sample in all cases was carried out in the range of 30–300°C at a rate of 10°C/min under a N_2 gas flow of 40 mL/min.

VI.2.3. Preparation of inclusion complex

The inclusion complex of SBZ and TSC4X was prepared using well-known co-precipitation method.[31] A mixed solution of TSC4X (30.8 mg, 4.0 mmol) and SBZ (90.5 mg, 4.0 mmol) in 1:1 molar ratio was prepared in 25 mL double distilled water. Then the mixed solution was stirred in a magnetic stirrer at 55°C for 48 hours till the emergence of a white precipitate. The white precipitate was filtered cautiously, and washed with ethanol followed by water for four times to eliminate uncomplexed SBZ and TSC4X. The resulting precipitate was then dried in a hot air oven at 50 °C for 12 hours. The obtained inclusion complex was kept in a dessicator prior to analysis.

VI.2.4. Preparation of 3D-structures of SBZ and TSC4X

The crystal structures of SBZ was collected from PubChem website (http://pubchem. ncbi.nlm.nih.gov). TSC4X was extracted from a complex with deposit number (CCDC ID : 246364) from Cambridge Crystal Data Centre (CCDC).[32] The missing

hydrogen atoms and atomic charges were added to TSC4X as well as SBZ, and energy minimization was carried out with DFT-B3LYP method using Gaussian 09 software.[33] These structures were used to perform the computational studies.

VI.2.5. Molecular docking study

Molecular docking is a computational process for predicting the predominant binding mode of a guest with a host.[34] An established docking protocol for host-guest system implemented in PyRx was applied.[35] Before conducting docking, PDB files of SBZ and TSC4X were converted into PDBQT format, and atomic coordinates were generated using PyRx docking software. The grid box center values were set as center_x= 6.0424, center_y= 3.6790 and center_z= 17.4442, and dimension values as size_x= 19.2728, size_y = 17.8871 and size_z = 17.3422 for all three coordinates. The grid box size was adjusted on binding pocket of TSC4X (receptor) to sufficiently allow SBZ (ligand) to move freely in the search space. Based on docking score, the lowest energy docked conformer, as visualized by PyMol software (Version 1.7.0, Schrodinger LLC., New York, NY, USA),[36] was selected.

VI.2.6. Aqueous solubility of SBZ-TSC4X complex

The aqueous solubility of SBZ-TSC4X complex was determined at 25°C.[37,38] Firstly, a sufficient quantity of SBZ-TSC4X complex was added to 5 ml water to ensure that the solution reached saturation. The solution at 25°C was shaken mechanically for 3 hours. Secondly, the solution was filtered using 0.45 μm Nylon Cameo syringe filter to remove remaining solid from the solution. The solubility or saturated concentration of SBZ-TSC4X complex in water was then measured using UV-Visible spectrophotometry.

VI.3. Result and Discussion

VI.3.1. Stoichiometric ratio evaluation of the inclusion complex by Job's method

A very reliable continuous variation method also known as Job's method was performed in order to validate the stoichiometry of the inclusion complex.[39] The sum of the concentrations of both components was kept constant ([SBZ]+[TSC4X] = 1.0×10^{-4} M) by varying the mole fraction of SBZ (R = [SBZ]/([SBZ]+[TSC4X])) from 0.0 to 1.0 (Table 1). In order to determine the stoichiometry of the inclusion complex, the UV-Visible absorption intensity variations of SBZ were plotted against the mole fraction (R).

Figure 1 illustrates the continuous variation spectra for the SBZ-TSC4X system (λ_{max} = 287 nm).[40] In Figure 2, the maximum was observed at mole fraction (R) = 0.5, which indicates 1:1 stoichiometry for the inclusion complex of SBZ and TSC4X.

VI.3.2. Absorption spectral analysis

The binding affinity of SBZ with TSC4X was established by determining association constant using UV-Visible absorption spectral studies.[41] The association constant (K_a) of SBZ-TSC4X inclusion complex at 298.15 K was determined from the noticeable increase in absorption intensity (ΔA) of SBZ (λ_{max} = 287 nm) with the increase in the TSC4X concentration by means of Benesi-Hildebrand equation (Table 2 and Figure 3). Based on Benesi-Hildebrand method, a double reciprocal plot for 1:1 inclusion complex is obtained using the following Benesi-Hildebrand equation

$$\frac{1}{\Delta A} = \frac{1}{K_a[SBZ]\Delta\varepsilon} \times \frac{1}{[TSC4X]} + \frac{1}{\Delta\varepsilon[SBZ]} \qquad (1)$$

where ΔA represents the difference in absorption intensity of SBZ in absence and presence of TSC4X. A double reciprocal plot (1/ΔA against 1/[TSC4X]) shown in Figure 4 demonstrates an excellent linear correlation (R^2 = 0.9992), confirming 1:1 complexation of SBZ with TSC4X.[39] The association constant (K_a) value, evaluated from double reciprocal plot by dividing intercept with slope, was found to be 6.01×10^3 M^{-1} (Table 3).

The binding free energy (ΔG) (Table 3) for the complex formation can be derived from association constant (K_a) value at 298.15 K using Gibb's equation (equation 2).

$$\Delta G = -RT \ln K_a \qquad (2)$$

The value of binding free energy (ΔG) was found to be -5.15 kcal/mol (Table 3), which suggest that the formation of SBZ-TSC4X complex is a spontaneous process.

VI.3.3. FT-IR spectral study

The study of SBZ-TSC4X inclusion complex can be carried out using FT-IR spectroscopic method. The formation of solid inclusion complex is supported by analyzing the changes in the peak position, shape, intensity and its disappearance in the spectra.[42] The IR spectra of SBZ, TSC4X and SBZ-TSC4X complex are shown in Figure 5, and the vibrational frequencies of the chemical bonds are listed in Table 4. In IR spectra

of SBZ, C=O stretching at 1697 cm^{-1}, aromatic ring stretching at 1556, 1490 cm^{-1}, aromatic C-H bending at 1265 cm^{-1}, aliphatic C-O stretching at 1073 cm^{-1} and SO_3H stretching at 1208 cm^{-1} were observed. In the case of TSC4X, the IR spectra is characterized by aromatic O-H stretching at 3353 cm^{-1}, aromatic skeletal C=C stretching vibrations at 1638, 1452 cm^{-1} and SO_3^- stretching vibrations at 1210, 1046 cm^{-1}. However, the IR peaks related to the C=O stretching, aromatic C=C stretching, aromatic C-H bending of SBZ were found to disappear and the aliphatic C-O stretching of SBZ was observed to appear at 1084 cm^{-1} in SBZ-TSC4X complex. Further, the vibrational bands corresponding to aromatic skeletal C=C stretching of TSC4X was observed at 1627, 1446 cm^{-1} in SBZ-TSC4X solid complex. Therefore, the observed disappearance and shifting of the vibrational modes of SBZ and TSC4X in SBZ-TSC4X complex indicates the encapsulation of unsubstituted aromatic moiety of SBZ into the cavity of TSC4X.

VI.3.4. Solubility study

The UV-Visible spectra of aqueous solutions of SBZ-TSC4X complex with different concentrations (pH = 7.0, 25°C) were shown in Figure 6(a). It can be observed that the absorbance increased with the concentration of SBZ-TSC4X complex. The absorbance of SBZ-TSC4X complex at 287 nm versus the concentration of SBZ-TSC4X complex was plotted, and a straight line was obtained as shown in Figure 6(b). According to the Lambert-Beer law, the absorption coefficient (ε) of SBZ-TSC4X complex in the aqueous solution (pH = 7.0, 25°C) was estimated as 0.6612 L g^{-1} cm^{-1}. Using the absorption coefficient (ε) value, the solubility of SBZ-TSC4X complex at 25°C in water was found to be 2.004 g L^{-1} (Figure 7). However, the reported solubility of pure SBZ at 25°C in water was 0.03 g L^{-1}.[43] Therefore, SBZ-TSC4X complex has higher solubility compared to SBZ. These results revealed that the encapsulation into TSC4X improved the aqueous solubility of SBZ.

VI.3.5. ^{1}H NMR spectral analysis

^{1}H NMR spectroscopy is a useful technique that can be utilized to explore the possible binding mode of guest molecule with TSC4X by analyzing the changes in chemical shift values (Δδ) of guest protons.[44,45] In the present work, the inclusion of SBZ into the cavity of TSC4X has been studied using ^{1}H NMR spectroscopy. The ^{1}H NMR spectra of pure SBZ, TSC4X and SBZ-TSC4X inclusion complex are shown in Figure 8

with their corresponding δ values in Table 5. After complex formation, H-1, H-2, H-3 protons of SBZ and Ar-O**H**, Ar-**H** protons of TSC4X were found to possess negligible changes in their δ values with $\Delta\delta_{complex-SBZ}$ 0.00, 0.01, 0.00 and $\Delta\delta_{complex-TSC4X}$ 0.01, 0.02 respectively. However, H-4, H-5 and H-6 protons of SBZ were observed to undergo visible upfield shifts with $\Delta\delta_{complex-SBZ}$ -0.04, -0.04 and -0.08 respectively. These changes in chemical shift values is due to the anisotropic ring-current effects of the aromatic nuclei of TSC4X, which indicates the encapsulation of unsubstituted aromatic moiety of SBZ into the TSC4X cavity. Since H-4, H-5 and H-6 protons were found to undergo considerable upfield shifts than H-1, H-2 and H-3 protons, therefore, it could be suggested that the unsubstituted aromatic moiety of SBZ is in close proximity to the aromatic nuclei of TSC4X (Scheme 2), which is in consonance with the observations obtained from FT-IR study.

VI.3.6. DSC analysis

The differential scanning calorimetry (DSC) is a thermodynamic tool for examining the thermal stability of a guest on complexation with a host.[46] The DSC analysis was carried out on SBZ, TSC4X and SBZ-TSC4X inclusion complex to validate the thermal stability of SBZ after its encapsulation into the cavity of TSC4X (Figure 9). The DSC curve of SBZ showed sharp melting endothermic peak at 145°C [Figure 9(a)]. TSC4X displayed a broader endothermal peak around 90°C in its thermogram, corresponding to the water loss [Figure 9(b)]. However, the endothermic peak at 145°C with much reduced intensity compared to that of pure SBZ was encountered for SBZ-TSC4X inclusion complex [Figure 9(c)]. Broader endothermal peak was encountered around 88°C for SBZ-TSC4X complex, indicating a dehydration process [Figure 9(c)]. These observations not only support the formation of SBZ-TSC4X inclusion complex, but also suggests that the thermal stability of SBZ has enhanced on inclusion complexation.

VI.3.7. ESI-MS studies

The prepared SBZ-TSC4X inclusion complex was analyzed using electrospray ionization mass spectroscopy (ESI-MS).[47] The characteristic peak observed at m/z 1214.13 corresponds to the molecular ion $[SBZ\text{-}TSC4X + H]^+$ and that at m/z 1236.19 corresponds to the molecular ion $[SBZ\text{-}TSC4X + Na]^+$ (Table 6 and Figure 10). This clearly supports the formation of stable SBZ-TSC4X inclusion complex with 1:1

stoichiometric ratio, which is in good agreement with the results obtained from Job's method.

VI.3.8. Molecular docking studies

The molecular docking has been extensively used to predict the binding orientation of a guest into the host cavity.[48] The docking has been carried out between SBZ and TSC4X using PyRx software. The best docked conformation of SBZ-TSC4X complex is shown in Figure 11 (a, side view ; b, top view). The lowest negative binding energy (ΔG) value for the most stable docked conformation of SBZ-TSC4X complex was found to be -4.40 kcal/mol (Table 7), which is very near to the value (≃ -5.15 kcal/mol for SBZ-TSC4X) obtained from UV-Visible spectroscopic studies, suggesting that the binding energy obtained from docking is in consonance with that derived from UV-Visible absorption analysis. Docking results demonstrated that in the docked conformation of SBZ-TSC4X complex (Figure 11), the unsubstituted aromatic moiety (i.e., phenyl ring) of SBZ was included into the hydrophobic pocket of TSC4X near the wider rim, while the substituted aromatic moiety of SBZ was found to present outside the wider rim of TSC4X cavity. Further, it can be observed that the docked conformation is stabilized by the π-π interactions between aromatic nuclei of TSC4X and unsubstituted aromatic moiety of SBZ (Figure 11). These interactions of SBZ with TSC4X obtained from docking study are in good agreement with the observations of ^{1}H NMR and FT-IR.

VI.3.9. Photostability evaluation

The photostability of pure SBZ and SBZ-TSC4X inclusion complex was examined using UV-Visible spectroscopic studies.[49] As shown in Figures 12 and 13, the initial absorbance of the solutions of both SBZ and SBZ-TSC4X inclusion complex was maintained at ~1 in the UVA and UVB regions (280–400 nm). Both of these solutions were then exposed to UV radiation for 100 minutes and the absorbance measurement (λ_{max} = 287 nm) of each of these solutions was carried out at 10 minutes interval. In case of pure SBZ, a reduction in absorbance of 25.9% was registered on irradiation over a period of 100 minutes with 10 minutes interval [Figures 12(a) and 13]. However, SBZ-TSC4X complex showed a reduction in absorbance of 18.4% on irradiation over a period of 100 minutes [Figures 12(b) and 13]. These observations suggest that the photostability of SBZ has improved on encapsulation with TSC4X.

VI.4. Conclusion

The molecular recognition of SBZ by TSC4X has been investigated. The Job's plot indicated that SBZ forms 1:1 inclusion complex with TSC4X, which was further supported by ESI-MS study. SBZ was found to possess higher binding affinity for TSC4X (K_a = 6.01×10^3 M^{-1}), and the negative free energy of binding (ΔG = -5.15 kcal mol^{-1}) suggested the binding process to be thermodynamically feasible. FT-IR and ^{1}H NMR studies demonstrated a preferential occupancy of the hydrophobic cavity of TSC4X by unsubstituted aromatic moiety of SBZ, which is in accordance with the docking analysis. DSC study showed that the complexation with TSC4X improved the thermal stability of SBZ. Finally, encapsulation of SBZ into the cavity of TSC4X also improved its photo-stability. Thus, the overall study concluded that SBZ-TSC4X supramolecular hybrid would enable the investigation of its applications as highly photo-stable sunscreen agent for cosmetic industry.

Tables

Table 1. Data for the Job plot performed by UV-Visible spectroscopy for aqueous SBZ-TSC4X system at 298.15K[a]

SBZ(ml)	TSC4X(ml)	SBZ (μM)	TSC4X (μM)	[SBZ]/([SBZ]+[TSC4X])	Absorbance(A)	ΔA	ΔA* [SBZ]/([SBZ]+[TSC4X])
0	4	0	100	0	0	0.6835698	0
0.4	3.6	10	90	0.1	0.51102745	0.17254235	0.017254235
0.8	3.2	20	80	0.2	0.53473523	0.14883457	0.029766914
1.2	2.8	30	70	0.3	0.55174562	0.13182418	0.039547254
1.6	2.4	40	60	0.4	0.57425983	0.10930997	0.043723988
2	2	50	50	0.5	0.59006421	0.09350559	0.046752795
2.4	1.6	60	40	0.6	0.61136452	0.07220528	0.043323168
2.8	1.2	70	30	0.7	0.62587152	0.05769828	0.040388796
3.2	0.8	80	20	0.8	0.64168432	0.04188548	0.033508384
3.6	0.4	90	10	0.9	0.66121687	0.02235293	0.020117637
4	0	100	0	1	0.6835698	0	0

[a]Standard uncertainties in temperature u are: u(T) = ±0.01 K.

Table 2. Data for the Benesi-Hildebrand double reciprocal plot performed by UV-Visible spectroscopy for aqueous SBZ-TSC4X system at 298.15 K[a] ; ± indicates the standard deviation

Temp (K)	[SBZ] (μM)	[TSC4X] (μM)	A_o	A	ΔA	1/[TSC4X] (M^{-1})	1/ΔA	Intercept	Slope	K_ax10^{-3} (M^{-1})
	10	10	0.475814	0.501675	0.025861	100000	38.66794			
	10	20	0.475814	0.521454	0.045639	50000	21.91086			
	10	30	0.475814	0.540155	0.06434	33333.33	15.54232			
	10	40	0.475814	0.560025	0.084211	25000	11.87498			

298.15	10	50	0.475814	0.576114	0.1003	20000	9.970124	2.23508	0.000372	6.01±0.74
	10	60	0.475814	0.596464	0.12065	16666.67	8.288444			
	10	70	0.475814	0.612545	0.13673	14285.71	7.313665			
	10	80	0.475814	0.626368	0.150554	12500	6.642151			
	10	90	0.475814	0.644726	0.168912	11111.11	5.920238			
	10	100	0.475814	0.668851	0.193037	10000	5.180353			

[a]Standard uncertainties in temperature u are: u(T) = ±0.01 K.

Table 3. The values of Association constant (K_a) and Gibb's free energy of binding (ΔG) at 298.15K for the inclusion complexation of SBZ with TSC4X in aqueous medium (1 kcal= 4.2 kJ)

Host	Guest	K_a (M^{-1})	lnK_a	ΔG^0(kcal/mol)
TSC4X	SBZ	6010	8.70	-5.15

Table 4. FT-IR data of pure SBZ, TSC4X and SBZ-TSC4X inclusion complex

SBZ	TSC4X	SBZ-TSC4X inclusion complex
1697 cm^{-1} : C=O stretching **1490, 1556 cm^{-1} :** aromatic C=C stretching **1265 cm^{-1} :** aromatic C-H bending **1073 cm^{-1} :** aliphatic C-O stretching **1208 cm^{-1} :** SO_3H stretching	**3353 cm^{-1} :** aromatic O-H stretching **1638, 1452 cm^{-1} :** aromatic skeletal C=C stretching vibrations **1210, 1046 cm^{-1} :** SO_3^- stretching	**1084 cm^{-1} :** aliphatic C-O stretching **1627, 1446 cm^{-1} :** aromatic skeletal C=C stretching

Table 5. ^{1}H NMR data of pure SBZ, TSC4X and SBZ-TSC4X inclusion complex in D_2O

	protons	ppm (D_2O)			Δδ = $\delta_{complex}$- δ_{SBZ}	Δδ = $\delta_{complex}$- δ_{TSC4X}
		δ_{SBZ}	δ_{TSC4X}	$\delta_{complex}$		
SBZ	H-1	6.45 (1H, s)	–	6.45 (1H, s)	0.00	–
	H-2	6.70-6.72 (1H, d, J= 8Hz)	–	6.71-6.73 (1H, d, J=8Hz)	0.01	–
	H-3	3.90 (1H, s)	–	3.90 (1H, s)	0.00	–
	H-4	7.74-7.76 (2H, dd, J= 8Hz)	–	7.74-7.70 (2H, dd, J=16Hz)	-0.04	–
	H-5	7.64-7.68 (2H, dd, J=16Hz)	–	7.64-7.60 (2H, dd, J=16Hz)	-0.04	–

	H-6	7.48-7.58 (m)	–	7.44-7.50 (m)	-0.08	–
TSC4X	Ar—O**H**	–	3.52 (4H, s)	3.53 (4H, s)	–	0.01
	Ar—**H**	–	7.78 (8H, s)	7.80 (8H, s)	–	0.02

Table 6. ESI-MS analysis of the SBZ-TSC4X complex with calculated as well as experimental mass

Name of the complexes	Calculated mass (a.u)	Experimental mass (a.u)
$[SBZ\text{-}TSC4X+H]^+$	1214.08	1214.13
$[SBZ\text{-}TSC4X+Na]^+$	1236.08	1236.19

Table 7. Binding affinity of SBZ with TSC4X obtained from Molecular Docking

Ligand with receptor	Binding affinity(ΔG) in kcal mol^{-1}
SBZ-TSC4X	-4.4

Figures

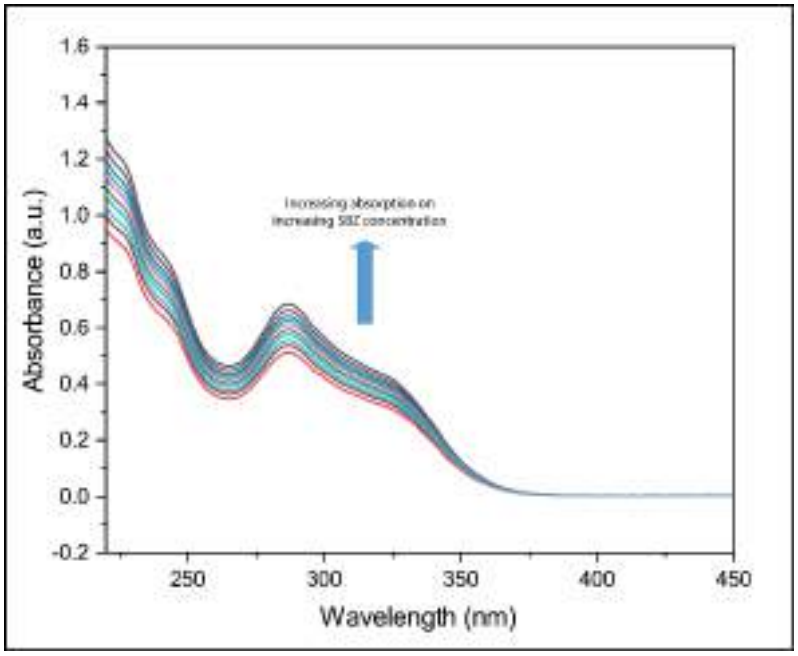

Figure 1. UV-Visible absorption spectra of SBZ by varying both host and guest concentrations such that the sum of the concentrations of both components was kept constant ([SBZ]+[TSC4X] = 1.0×10^{-4} M).

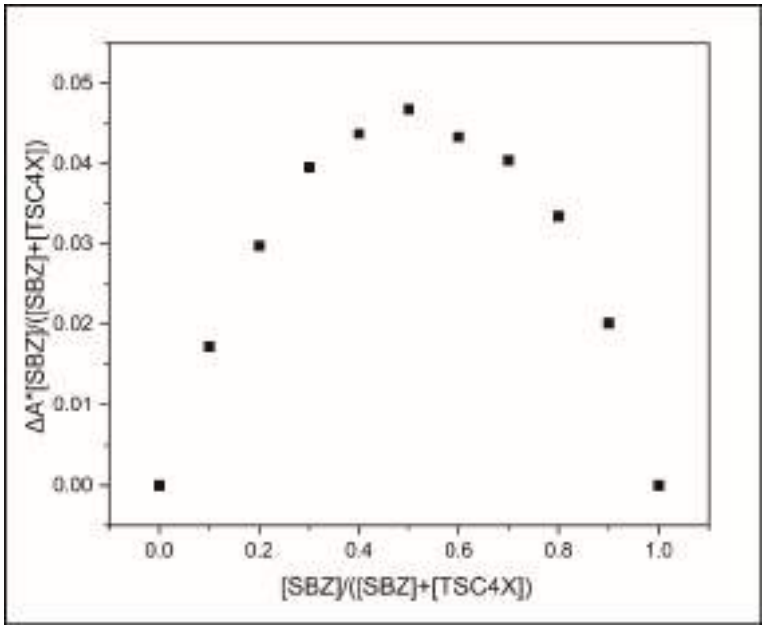

Figure 2. Job's plot for SBZ-TSC4X system at 298.15 K (λ_{max} = 287 nm).

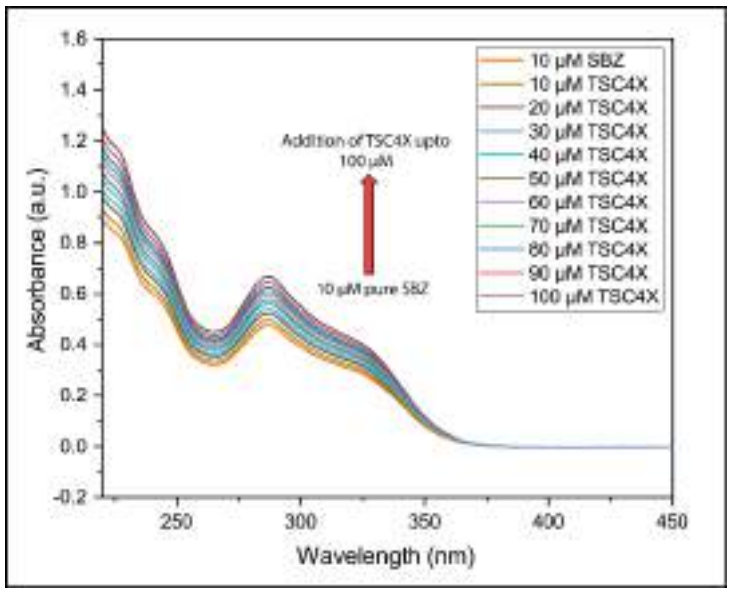

Figure 3. UV absorption spectra of SBZ in the absence and presence of various concentrations of TSC4X at 298.15 K; where, initial concentration of SBZ was 10 μM and variations of concentration of TSC4X started from 10 μM, 20 μM, 30 μM upto 100 μM.

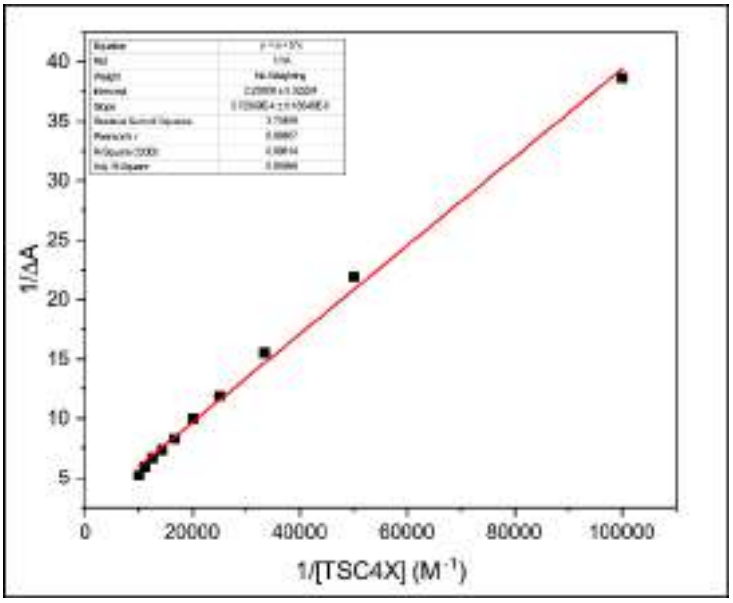

Figure 4. Double reciprocal Benesi-Hildebrand plot of 1/ΔA versus 1/[TSC4X] at 298.15 K.

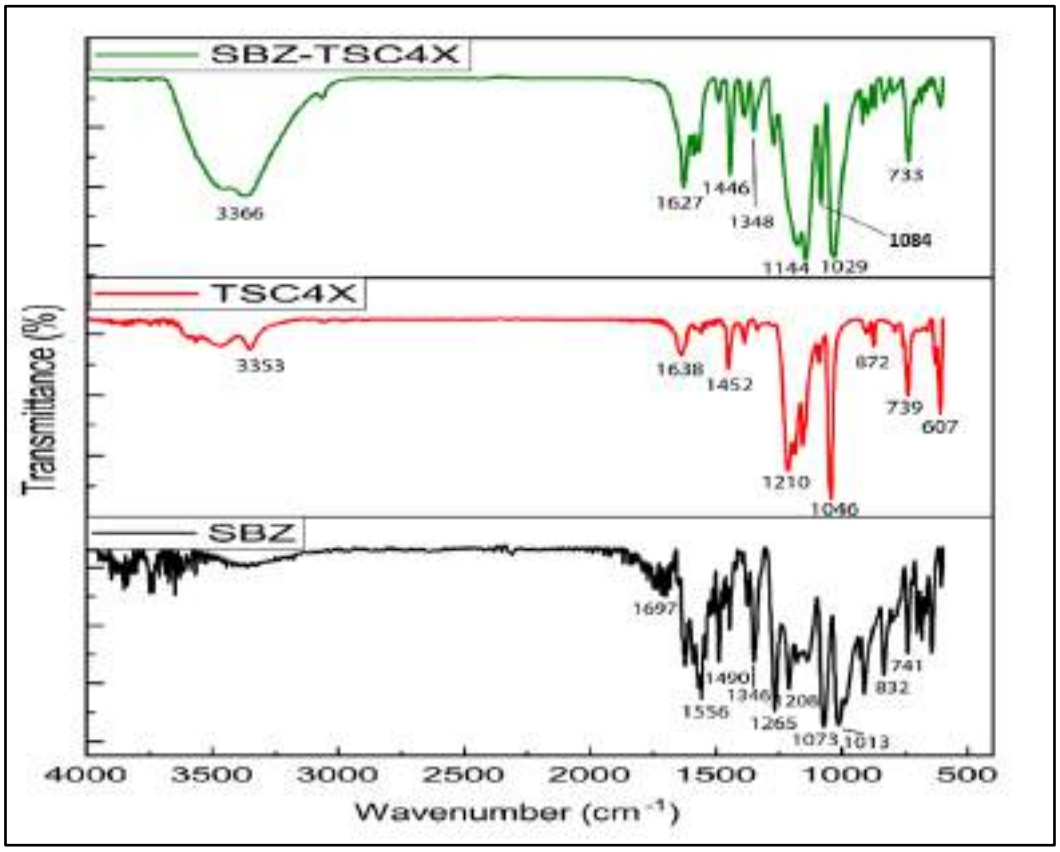

Figure 5. FT-IR spectra of SBZ, TSC4X and SBZ-TSC4X inclusion complex.

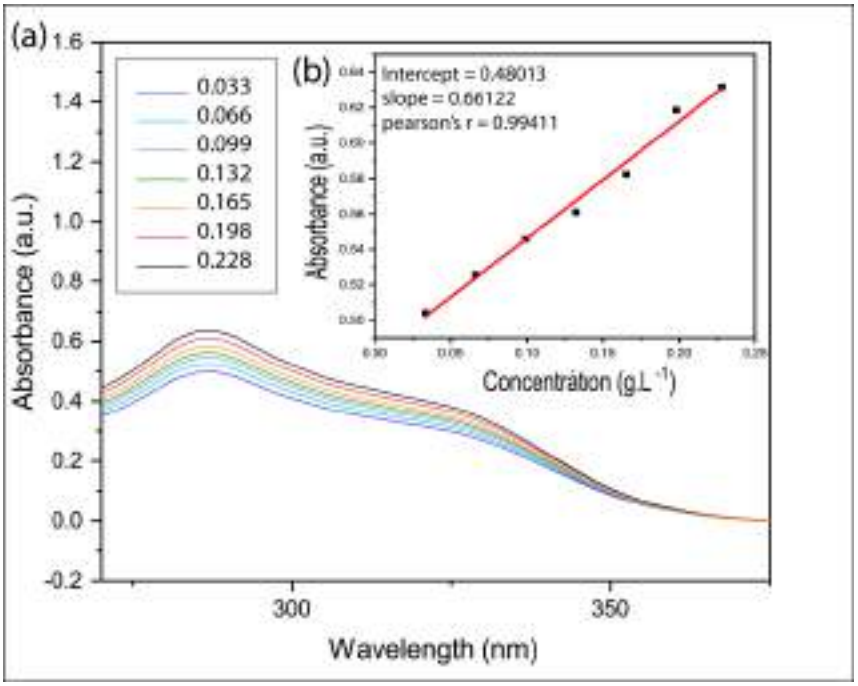

Figure 6. (a) UV-Visible spectra of SBZ-TSC4X complex with different concentrations (g L^{-1}) in aqueous solution (pH = 7.0, 25°C). **(b)** A plot of absorbance of SBZ-TSC4X complex at 287 nm versus the concentration of SBZ-TSC4X complex.

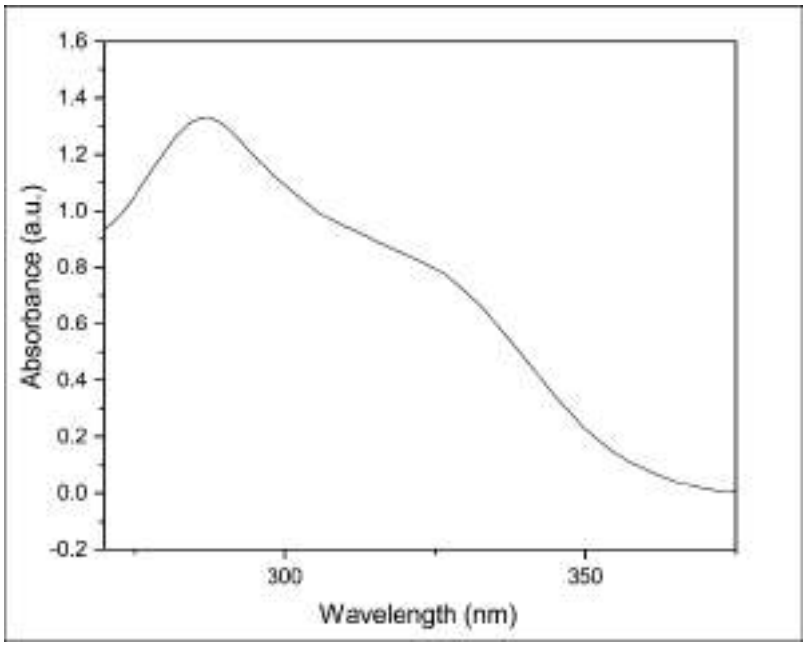

Figure 7. UV-Visible spectra of SBZ-TSC4X saturated aqueous solution.

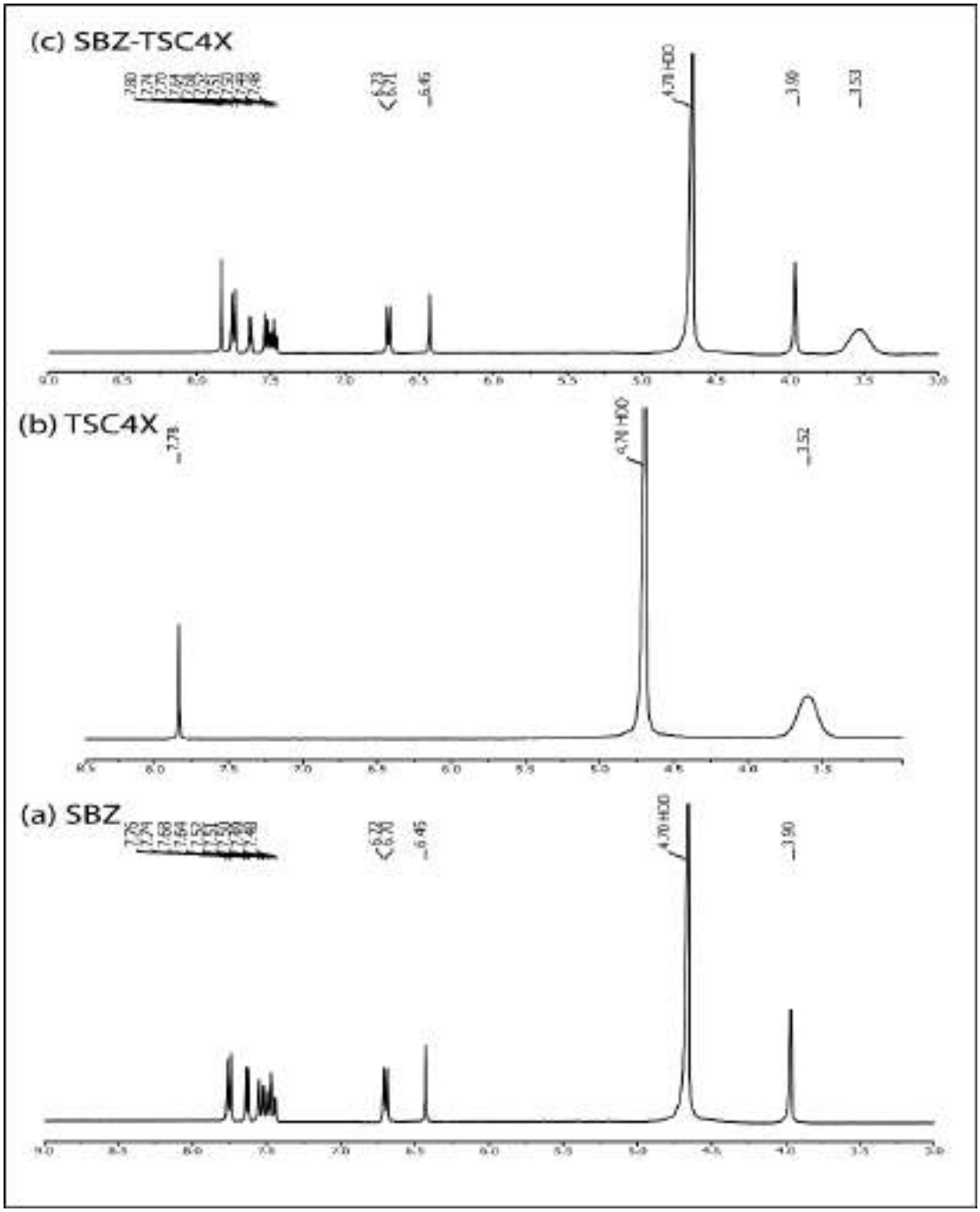

Figure 8. ^{1}H NMR spectra of **(a)** SBZ, **(b)** TSC4X and **(c)** SBZ-TSC4X inclusion complex.

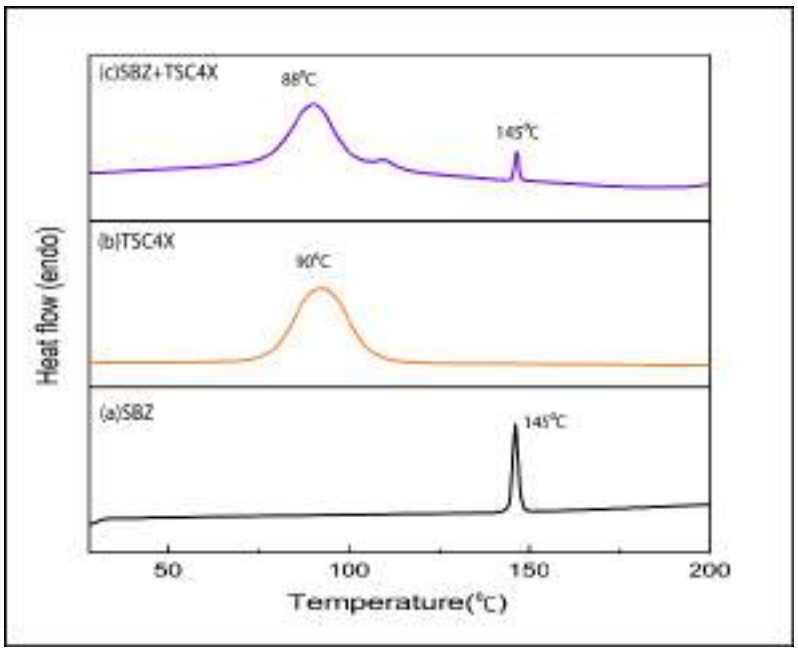

Figure 9. DSC thermograms of **(a)** SBZ, **(b)** TSC4X and **(c)** SBZ-TSC4X inclusion complex.

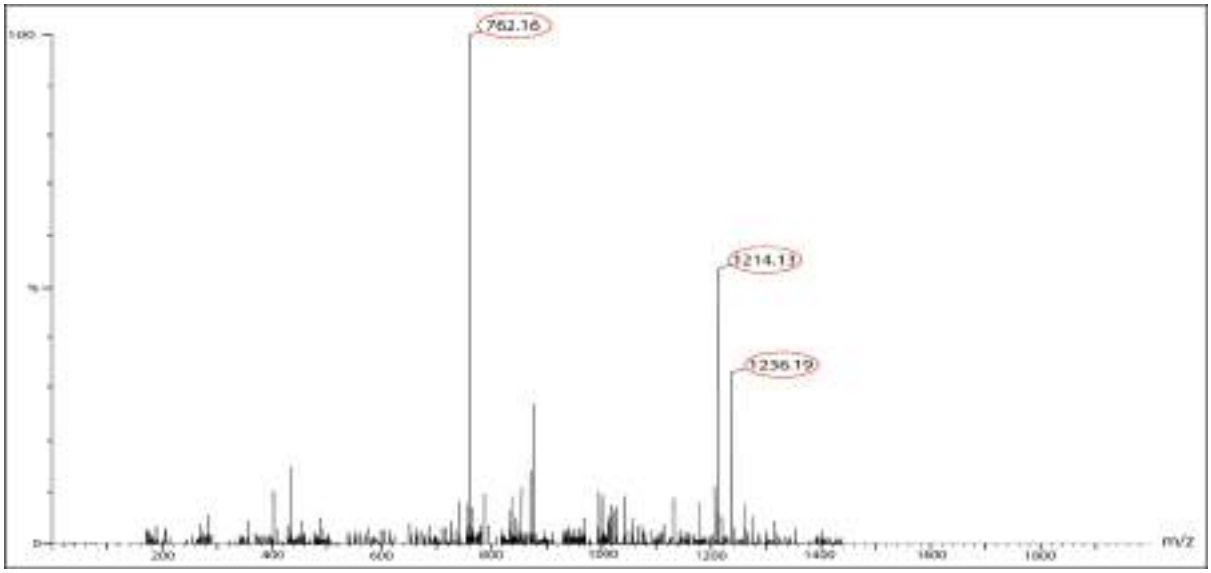

Figure 10. ESI mass spectra of SBZ-TSC4X inclusion complex.

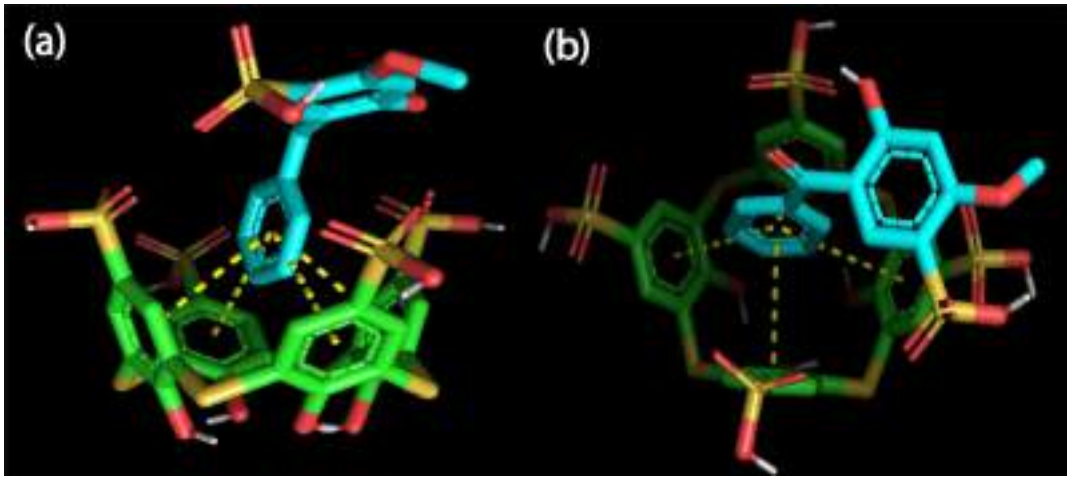

Figure 11. Best conformational model of SBZ-TSC4X inclusion complex, side view **(a)** and top view **(b)**.

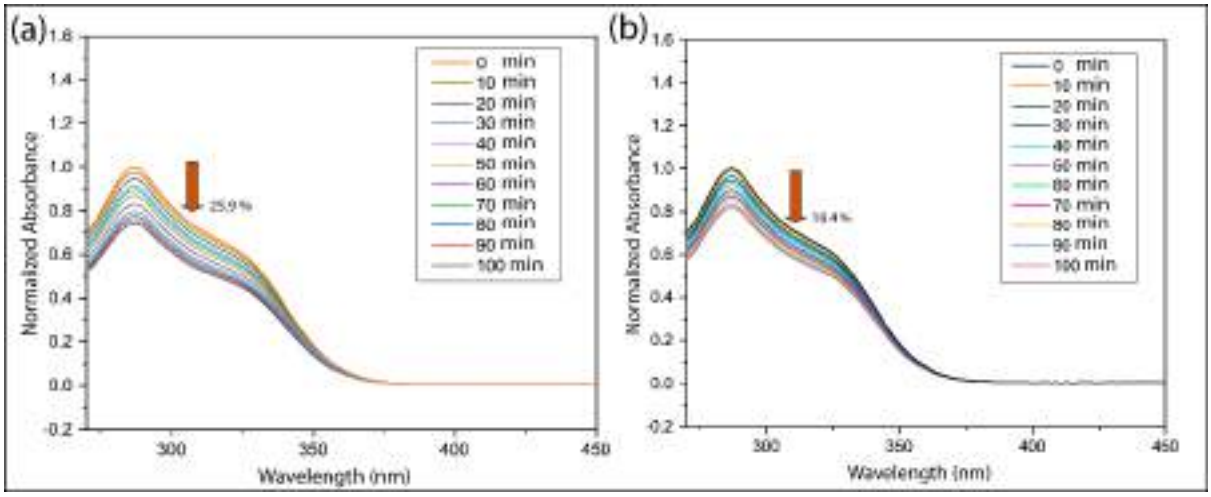

Figure 12. Absorption spectra of **(a)** SBZ and **(b)** SBZ-TSC4X complex recorded at different time intervals during UV irradiation.

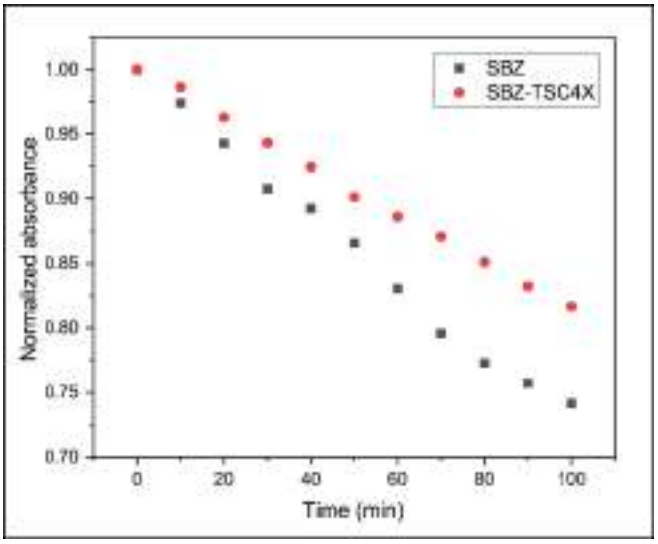

Figure 13. Normalized absorbance change over a period of time in minutes.

Schemes

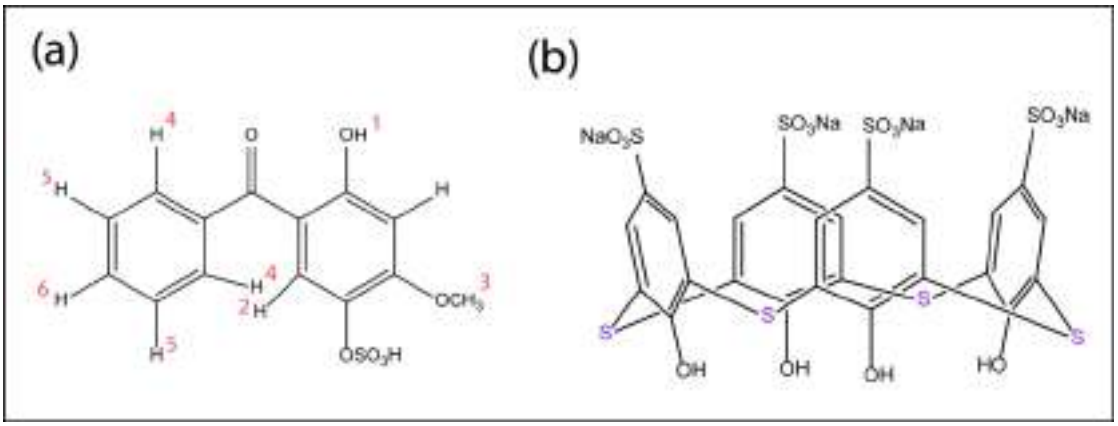

Scheme 1. The two dimensional structure of **(a)** sulisobenzone and **(b)** *p*-sulfonatothiacalix[4]arene (TSC4X).

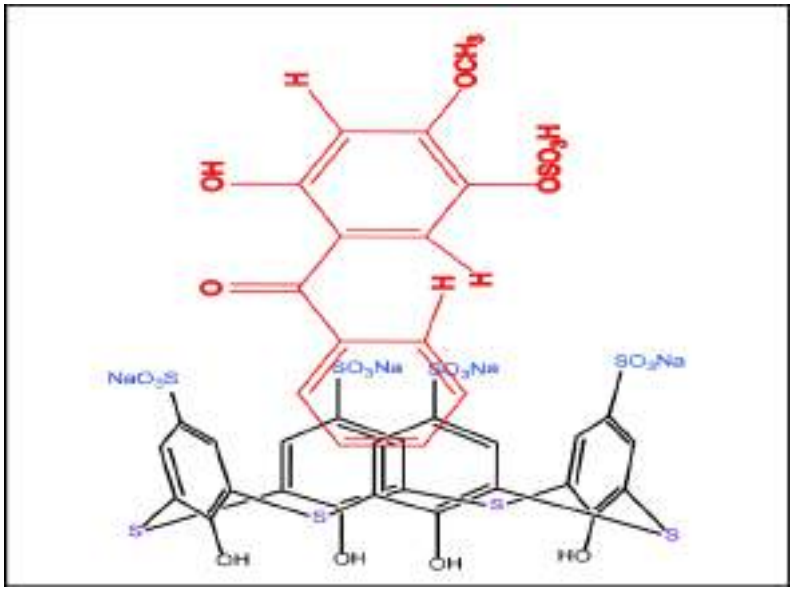

Scheme 2. Illustration of the complexation between SBZ and TSC4X molecule.